REGULATION OF REPRODUCTIVE PROCESSES WITH DYNAMIC ENERGY BUDGETS

Erik B. Muller[1,2*], Konstadia Lika[3], Roger M. Nisbet[4], Irvin R. Schultz[5], Jérôme Casas[6], André Gergs[7,8], Cheryl A. Murphy[9], Diane Nacci[10], Karen H. Watanabe[11]

[1]Department of Biology. Norwegian University of Science and Technology, Trondheim, Norway

[2]Marine Science Institute, University of California, Santa Barbara, CA, USA

[3]Department of Biology, University of Crete, Heraklion, Greece

[4]Department of Ecology, Evolution and Marine Biology, University of California, Santa Barbara, CA, USA

[5]Pacific Northwest National Laboratory, Marine Sciences Laboratory, Sequim, WA, USA.

Current Address: Lynker Technologies under contract to Northwest Fisheries Science Center, National Marine Fisheries Service, National Oceanic and Atmospheric Administration, Seattle, WA, USA.

[6]Institute de Recherche sur la Biologie de l'Insecte, Université de Tours, Tours, France

[7]gaiac - Research Institute for Ecosystem Analysis and Assessment, Aachen, Germany

[8]current affiliation: Bayer AG, Monheim, Germany

[9]Department of Fisheries and Wildlife, Michigan State University, East Lansing, MI, USA

[10]US Environmental Protection Agency, Office of Research and Development, Narragansett, RI, USA

[11]School of Mathematical and Natural Sciences, Arizona State University, Glendale, AZ, USA

[*]Corresponding author erik.muller@lifesci.ucsb.edu , bpbleus@yahoo.com

KEYWORDS

Dynamic Energy Budget; DEB theory; Bioenergetics, Rainbow trout

ABSTRACT

1. Linking organismal level processes to underlying suborganismal mechanisms at the molecular, cellular and organ level constitutes a major challenge for predictive ecological risk assessments. This challenge can be addressed with the simple bioenergetic models in the family of Dynamic Energy Budget (DEB), which consist of a small number of state equations quantifying universal processes, such as feeding, maintenance, development, reproduction and growth.
2. Motivated by the need for process-based models to evaluate the impact of endocrine disruptors on ecologically relevant endpoints, this paper develops and evaluates two general modeling modules describing demand-driven feedback mechanisms within the DEB modeling framework exerted by gonads on the allocation of resources to production of reproductive matter.
3. These modules describe iteroparous, semelparous and batch-mode reproductive strategies. The modules have a generic form with both positive and negative feedback components; species and sex specific attributes of endocrine regulation can be added without changing the core of the modules.
4. We demonstrate that these modules successfully describe time-resolved measurements of wet weight of body, ovaries and liver, egg diameter and plasma content of vitellogenin and estradiol in rainbow trout (*Oncorynchus mykiss*) by fitting these models to published and new data, which require the estimation of less than two parameters per data type.
5. We illustrate the general applicability of the concept of demand-driven allocation of resources to reproduction by evaluating one of the modules with data on growth and seed production of an annual plant, the common bean (*Phaseolis vulgaris*).

Introduction

Dynamic Energy Budget (DEB) theory offers a remarkably general mathematical and conceptual framework for physiological ecology. Originally formulated to describe growth and reproduction in animals, DEB theory now describes widespread empirical patterns in metabolic behavior of a steadily increasing number species (over 1,200 at the time of writing) from phyla from all three domains (Sousa, Domingos & Kooijman 2008; Kooijman 2010; Jusup *et al.* 2017; AmP 2018). Its core concepts are consistent with some general trends in evolutionary history (Kooijman 1986; Kooijman & Troost 2007) and with the principles of thermodynamics (Sousa *et al.* 2010; Jusup *et al.* 2017). In addition, the theory offers a powerful framework for modeling organismal response to environmental stress, notably in ecotoxicology (Kooijman & Bedaux 1996; Jager *et al.* 2014; Muller *et al.* 2014) and, more recently, in the context of ocean acidification (Muller & Nisbet 2014; Jager, Ravagnan & Dupont 2016), starvation (Gergs & Jager 2014) and crowding stress (Gergs, Preuss & Palmqvist 2014). The versatility of the theory is due to its modular structure, through which specific attributes or 'details' of a particular environment, stressor or species can be included without changing the core of the model. Here we follow a similar approach to accommodate life history strategies by which organisms allocate resources to reproduction. Since reproduction generally constitutes a major fraction of the total energy budget of an adult organism, the energetic implications of different reproductive strategies and their trade-offs play a fundamental role in life history theory (Stearns 1992).

An important feature of most DEB models is that resources are first assimilated into somatic reserves, which are then committed to support somatic, developmental and/or reproductive functions, depending on nutritional status and life stage. In the standard formulation of DEB (stdDEB), applicable to animals, the rate at which reserves are allocated to reproduction depends

71 only on the reserve density and the size of the animal (see Figure 1). Control mechanisms
72 regulating the partitioning of reserves to favor growth over reproduction, or *vice versa*, are
73 absent. Standard DEB ignores control mechanisms regulating the development of gonads, as the
74 specifics of those mechanisms vary widely among taxa and sexes (but see Pecquerie, Petitgas
75 and Kooijman (2009), Einarsson, Birnir and Sigurosson (2011), Augustine *et al.* (2012) and
76 Llandres *et al.* (2015) for species or group specific DEB gonad loading modeling modules for
77 anchovy, capelin, zebrafish and parasitic wasps, respectively). This lack of feedback simplifies
78 the dynamics of resource allocation, with obvious mathematical advantages as a result. Yet,
79 stdDEB quantifies reproductive output sufficiently accurately for many purposes, such as those
80 that require estimates of reproductive output over longer time spans or those involving species
81 that release gametes in a nearly continuous manner. However, it is important to consider
82 feedback, e.g., mediated by endocrine regulation mechanisms, in order to capture the *dynamics*
83 of gamete maturation in iteroparous and semelparous organisms, in which gametes mature
84 during the later part of the reproductive cycle or near the end of the life cycle, respectively. In
85 addition, this kind of feedback could provide an entry to mechanistic modeling of the impact of
86 endocrine disruptors on growth and reproduction in the DEB framework.
87 To more accurately accommodate the alternative reproductive strategies of iteroparous and
88 semelparous organisms, we develop and evaluate the performance of two extensions of the
89 standard DEB model. These extensions include demand-driven feedback mechanisms on gonad
90 development, guided by the premise that hormones produced in the reproductive organs and
91 other organs commonly mediate those feedback mechanisms. We center our evaluation of model
92 performance on a single fish species, the rainbow trout (*Oncorynchus mykiss*), due to the
93 expansive data set on its growth and reproductive biology. However, we argue that the model

extensions are based on general principles, and therefore applicable to other species. As an illustration, we discuss how simplified formalism from one of the model extensions can be applied to describe the growth and reproductive patterns in a species very different from trout, namely the common bean (*Phaseolis vulgaris*). Beans have a reproductive strategy typical for many annual plants, namely an allocation strategy that favors seed production over somatic growth during the later phases of the life cycle. In addition, we discuss how these extensions can be useful in exploring physiological mechanisms by which stressors, in particular endocrine disruptors, affect resource allocation, and ultimately adverse outcomes to reproduction and growth.

Materials and methods

DATA SOURCES

Three data sets about female rainbow trout (*O. mykiss*) were analyzed to evaluate model performance. The most expansive set, referred to as main data set, was from Nagler *et al.* (2012) with additional data from Gillies *et al.* (2016), and concerns a reproductively synchronized autumn-spawning population obtained from a commercial supplier (Troutlodge, Inc., Sumner, WA) and maintained in a temperature controlled flow-through system under a natural lighting regime at the Battelle Marine Science Facility (Sequim, WA). The main data set included time-resolved measurements of wet weight of body, ovaries and liver, egg diameter and plasma content of vitellogenin and estradiol of 58 individuals. The two supplementary data sets, SD1 and SD2, were more limited in scope. SD1 included time resolved measurements of body weight and egg mass of 12 and 9 individuals, respectively, of a spring spawning strain obtained from Troutlodge Inc. (Sumner, WA). SD2 included initial and final total body and egg weights as well

as weights and diameters of individual eggs of 16 individuals of a fall-spawning strain obtained from Nisqually Trout Farm (Lacey, WA). Fish of SD1 and SD2 were kept in the same facility as those of the main set; see Nagler *et al.* (2012), Schultz *et al.* (2013) and the Supplemental Information for experimental detail. All sets span a single breeding cycle of approximately 11-14 months starting immediately after the time of first spawning.

The common bean, *Phaseolis vulgaris*, was used to evaluate the potential of the principle of demand driven resource allocation to reproduction (see next section) to capture the dynamics of growth and reproduction of a species wildly different from iteroparous rainbow trout; beans have a semelparous reproductive strategy typical for many annual plants, namely an allocation strategy that favors seed production over somatic growth during the later phases of the life cycle. Data are from Lima *et al.* (2005) and include time-resolved measurements of vegetative above ground biomass, leaf cover and pod biomass of 6 cultivars grown in a field setting in coastal Brazil from May to August (mean growing conditions: 21.2^{o}C, 70% humidity, 6.9 h solar radiation per day; 12 seeds per row meter at 0.5 m row distance; plots fertilized with 2.5 g N, 4.0 g P and 4.0 g K per square meter).

DYNAMIC ENERGY BUDGET THEORY

This study uses the standard model of Dynamic Energy Budget (stdDEB) theory as a reference. Since Kooijman (2010) has described this theory and its standard formulation in detail and several other publications provide extensive summaries (Nisbet *et al.* 2000; Sousa, Domingos & Kooijman 2008; Jusup *et al.* 2017), we only present features of the theory that are essential to evaluate the models developed in this study.

139 The stdDEB formulation (see Fig. 1), describes the rates at which a 'generalized' animal acquires
140 resources from its environment and uses the energy therein for somatic and maturity
141 maintenance, growth, maturation (juveniles) and reproduction (adults). A 'generalized' animal is
142 heterotrophic, grows isometrically (constant shape), does not encounter conditions of stress
143 (including debilitating forms of starvation), and has three life stages: embryonic (during which it
144 does not feed), juvenile (feeding but no reproduction) and adult. Since this study involves the
145 adult stage only, from now on, all references to animals pertain to adults, unless other life stages
146 are explicitly mentioned. stdDEB distinguishes three pools of biomass: structure, general reserve
147 and material in the reproductive buffer. Structure is defined as the biomass requiring
148 maintenance in order to remain viable. The reproductive buffer contains resources tagged for
149 reproduction (irreversibly, except potentially during starvation conditions). General reserve is
150 functionally defined as all other metabolizable biomass; in practice, general reserve typically
151 includes conventional storage materials as well as compounds that are traditionally not thought
152 of as reserve, such as ribosomes in excess of the minimal amount needed to ensure vitality of an
153 organism of a given size (Nisbet *et al.* 2000). The gross biochemical composition of each pool is
154 considered to be invariant, implying that the costs to produce a unit of each type of biomass and
155 the cost to maintain a unit of structure are constant. The general reserve density, i.e., the ratio of
156 general reserve and structure, stabilizes in a constant food environment.
157 Environmental resources are first assimilated into general reserve, which is subsequently
158 committed to somatic and developmental/ reproductive functions, with each set of functions
159 receiving a constant fraction κ of committed general reserve (see Figure 1). In order to
160 accommodate the changing rate of gamete development during a reproductive cycle in female
161 rainbow trout, we studied two extensions to the standard model (see Figure 1). In the first

variant, the proportion of committed general reserve allocated to reproduction is subject to feedback regulation of the reproductive buffer, implying that the allocation of general reserve to reproduction is driven by demand of the reproductive buffer. This variant is denoted dDEB, with the '*d*' standing for 'demand-driven'. The second variant, a modified version of a capelin model by Einarsson, Birnir and Sigurosson (2011), assumes stdDEB but separates the reproductive buffer in pools of unspecified reproductive reserve and actual reproductive matter. A gonad loading modeling module describes the rate at which reproductive reserve are converted into actual reproductive matter. This variant will be denoted stdDEB+, with the '+' referring to the gonad loading module. Regulation of the allocation of reserves to the reproductive buffer in dDEB and of gonad loading in stdDEB+ are subject to endocrine control.

The derivations of the dDEB and stdDEB+ model equations in Table 1 are presented in full in the Supplementary Information. Here, only the assumptions that are not part of stdDEB are presented and evaluated. The following list contains assumptions shared by and specific to both model variants, though it should be stressed that reproductive matter is defined differently in those variants. In dDEB, reproductive matter refers to all matter in the reproductive buffer regardless of location in the body, whereas reproductive matter roughly corresponds to gametes in stdDEB+. The assumptions are:

1. At the onset of a reproductive cycle, a small fraction of somatic biomass is converted to reproductive matter, e.g., due to meiosis. General reserve and structure contribute proportionally to the initial formation of reproductive matter, and the costs of this conversion are negligible. The latter two assumptions are rather arbitrary but quantitatively insubstantial.

2. The initial density of reproductive matter is constant. This assumption maintains parameter parsimony and model simplicity.
3. An adult has a bounded capacity to carry reproductive matter. In non-starving adults, this capacity is proportional to the amount of structural biomass, i.e., the maximum density of reproductive matter is a constant. This assumption maintains parameter parsimony and model simplicity.
4. dDEB only: the fraction of mobilized general reserve allocated to reproduction and maturity maintenance in adults is proportional to (1) the density of reproductive matter, and (2) the difference between the maximum and actual density of reproductive matter. The first proportionality introduces positive feedback and is based on the general observation that the ovaries in fish produce estrogen, which stimulates the production of vitellogenin, the precursor of egg reserve material (Tyler & Sumpter 1996). The second proportionality provides a simple negative feedback (i.e., deceleration) mechanism that causes the accumulation of reproductive material in the gonads to slow down towards the end of a reproductive cycle.
5. stdDEB+ only: the rate at which reproductive reserves are converted to reproductive matter is proportional to (1) the density of reproductive reserves, (2) the density of reproductive matter, (3) the difference between the maximum and actual density of reproductive matter, and (4) the amount of structural biomass. The first proportionality ensures the density of reproductive reserves cannot become negative; for arguments for the two subsequent proportionalities, see previous assumption.
6. The efficiency with which reproductive reserves are converted into reproductive matter is constant.

7. Spawning requires the density of reproductive matter to exceed a threshold and, additionally, may be under the control of a time trigger or environmental factor, depending on species.

LINK BETWEEN DEB QUANTITIES AND DATA

Variables in DEB models are abstract quantities and therefore do not correspond directly with measurable quantities. The mapping of DEB quantities onto the data analyzed in this study, including total body, ovary and liver wet weights, follicle diameter and plasma levels of estradiol and vitellogenin, is achieved through auxiliary assumptions stated in this section; the corresponding equations, summarized in Table 1, are derived in the Supplementary Information. The relationship between measurable quantities pertaining to the common bean and those of a DEB model of bean growth and fecundity can be found in the Supplementary Information.

In order to convert DEB mass quantities to wet weights, we use conversion factors from the rainbow trout entry in the DEB parameter database (Kooijman *et al.* 2017). Considering that the ovaries mainly consist of storage materials in eggs, we assume the contributions of structure and general reserves to the wet weight of the ovaries are negligible (to avoid confusion, we will use 'storage' to refer to physical materials and 'reserves' as the conceptual abstraction in the context of DEB). We also assume that the fraction of reproductive matter that is in the ovaries is constant. Furthermore, we assume that reproductive matter is either in the ovaries or in the liver, which produces the precursors of egg storage materials. It is prudent to consider also including plasma vitellogenin, the precursor of egg storage materials. However, plasma vitellogenin levels are especially high just prior and after ovulation, indicating that not all plasma vitellogenin ends up in eggs. Furthermore, the fraction of vitellogenin in plasma is relatively small. Plasma contributes 2.5% to 5.5% to body wet weight in teleost fish (Brill *et al.* 1998, and references

therein) and contains about 25 mg vitellogenin/ ml during the phase of accelerating ovary growth in a typical individual in this study (see figure 2F), which corresponds to only about 1.5-3.5 g vitellogenin in a 2.5 kg fish. Thus, it is reasonable to ignore the contribution of vitellogenin to reproductive matter, though its dynamics are informative and are modeled later. Furthermore, we assume that the fractions of structure and reserves that are part of the liver are constants for both model variants, and, for stdDEB+, in order to retain simplicity, that the amount of reproductive reserves in the liver is negligible.

This leaves the follicle diameter and estradiol and vitellogenin plasma levels as the experimental quantities that need to be related to DEB variables. In order to relate the mean diameter of a follicle to reproductive matter, we assume that follicles are perfect spheres and that the specific gravity of biomass equals unity. Estradiol is produced by the ovaries and regulates the flow of vitellogenin to the ovaries. Accordingly, we link the gonad loading module of stdDEB+ and the reproduction flux in dDEB to the plasma estradiol concentration assuming simple proportionality.

To model the dynamics of plasma vitellogenin, we assume that the volume of plasma is proportional to the amount of structural biomass, and that the rate at which vitellogenin is cleared from plasma is proportional to the amount of structural biomass (e.g., by structural mass in the ovaries). Furthermore, for dDEB, we assume that the rate at which vitellogenin is released into the blood stream is proportional to the rate at which somatic reserves are allocated to reproduction. For stdDEB+, we assume that the rate at which vitellogenin is released into the blood stream is proportional to the rate at which reproductive reserves are allocated to reproductive matter.

PARAMETERIZATION

In the evaluation of model performance with trout data, the values of some or all parameters in Table 2 were fixed, depending on the information content of the data and on the purpose of the analysis (see legend to Figure 4 for information about parameter values regarding the analysis of bean data). The main data set was used to parameterize the model variants; subsequently, this parameterization was used to predict the observations in the supplementary data sets SD1 and SD2 (with one exception – see next section). However, not all parameters were estimable from the main data set due to a lack of information about, e.g., elemental biomass composition and some conversion efficiencies, and therefore had to be fixed; similar values were used for fixed parameters that occur in both model variants. The values of eight fixed parameters, as marked in Table 2c, were taken or calculated from the rainbow trout entry in the DEB parameter database (Kooijman *et al.* 2017). Among those was the somatic maintenance rate parameter, which could not be estimated as it strongly covaried with other parameters, notably the general reserve turnover rate. Since the value of the somatic maintenance rate parameter is relatively invariant across species (Kooijman 2010), it was fixed at the value in the DEB parameter database, while the latter was treated as a free parameter.

The reasoning for the remaining five fixed values is as follows. First, the value for the scaled food density was set at 0.9, which is close to its maximum of 1.0, as the fish were well fed. Second, according to the parameter database, maturity maintenance costs would have been an insubstantial fraction of the total energy budget of the fishes and were therefore ignored. Third, the initial density of reproductive reserve in stdDEB+ was assumed negligible, since there was no information available that could be used to identify the reproductive reserve pool as a pool

276 separate from general reserve and reproductive matter in this model variant (in contrast, this
277 parameter could be estimated for dDEB – see Table 2d). This assumption is supported by the fact
278 the fish had recently matured and were stripped before the experiment. Fourth, the maximum
279 density of reproductive matter in stdDEB+ strongly covaried with other parameters and was
280 therefore fixed; it was identical to the density of reproductive matter in a female of ultimate size
281 at optimal conditions after one year according to the parameter database. Fifth, the conversion
282 efficiency of reproductive reserves to reproductive matter in stdDEB+ was set at unity, implying
283 that all the conversion overheads were subsumed in the conversion of general into reproductive
284 reserve.
285 Free parameters were estimated by maximizing likelihood considering all data types in a set
286 simultaneously, while assuming that discrepancies between data and model predictions were due
287 to normally distributed homoscedastic error in the data. These estimations were done with a
288 modified version of the BYOM platform coded in Matlab (www.debtox.info/byom). Confidence
289 intervals were estimated from the likelihood profile of each parameter. Universally suitable
290 goodness-of-fit measures are lacking for nonlinear models (see e.g. Shcherbakov *et al.* 2013),
291 which problem was compounded by the composite nature of the trout data sets analyzed in this
292 study. Therefore, in the analysis of trout data sets, in addition to likelihood values, two goodness-
293 of-fit measures were used to evaluate model performance: the symmetric mean scaled error,
294 $SMScE_i$, and the model efficiency, ME - see Supplemental Information for equations.
295

296 ## Results

297 The dDEB and stdDEB+ models are relatively parameter sparse. The dDEB model needed 21
298 parameters, of which 12 were estimated, to describe the patterns in the main data set by Gillies *et*

al. (2016), including total body, ovaries, total body less ovaries and liver wet weight, mean follicle diameter and vitellogenin and estradiol plasma content. The stdDEB+ model required two more parameters, 23 in total, of which 11 could be estimated from the main data set. Thus, on average, less than two parameters were estimated from each data type.

Despite this relative parameter sparseness, both models fit the trends in the main data set well (see Figure 2 and Table 2). The fits to the weight and follicle diameter data are virtually indistinguishable between the two models (see Figure 2A-E). The goodness-of-fit measures are also similar for the two models (see Table 2). In addition, the estimated values for the general reserve turnover rate k_E, the only free core DEB parameter, are statistically indistinguishable at the 95% level (see Table 2d), though the value implied by the parameters published in the DEB parameter database for rainbow trout (Kooijman *et al.* 2017) is about 10-20% lower ($2.92\ 10^{-3}$ day^{-1} at 11°C). More divergence in model performance is seen in the predictions of plasma vitellogenin and estradiol contents, notably during the last third of the reproductive cycle (see Figure 2F-G). The peaks of those plasma contents in this period are substantially better described by dDEB than by stdDEB+, as the latter cannot capture the drop in plasma vitellogenin and estradiol levels near the end of the reproductive cycle. The goodness-of-fit measures for those plasma contents also favor dDEB over stdDEB+ (see Table 3). In addition, the overall goodness-of-fit measures point to dDEB as the superior model. The AIC criterion also points to dDEB as the preferable model, since the log likelihood of dDEB is 21.9 higher than that of stdDEB+, which is a large difference, especially given that dDEB has only one more free parameter than stdDEB+.

Although cultivation conditions were roughly similar among the three experiments, the fish in the supplementary data sets SD1 and SD2 grew more vigorously than those in the main data set.

This can be clearly seen in Fig. 3A, which shows that the model predictions by dDEB and stdDEB+ with the parameters estimated from the main data set (bottom two curves) underestimate growth of fish in set SD1. The predictions are greatly improved, however, by adjusting the general reserve turnover rate parameter. Increasing this value by 25% (dDEB) or 20% (stdDEB+) yields curves that are virtually indistinguishable and represent the growth data well. Similarly, with the value of the general reserve turnover rate parameter from the main data set, both models estimate the predictions of end weights in data set SD2 about 25-30% lower than actually observed. Also with this data set, satisfactory estimates of final body weights are obtained by increasing the value of the general reserve turnover rate parameter with 35% (dDEB) or 20% (stdDEB+) (results not shown).

The analysis of reproductive data from SD1 and SD2 comes with two caveats. First, the exact moment of spawning in these experiments is unknown. This hinders the comparison of model predictions of reproductive endpoints with observed values, as the former depend strongly on timing, given the relatively steep increase in ovary weight during the final weeks of the reproductive cycle (*cf.* Fig 2C). Second, the models predict the weight of ovaries, whereas the data report egg mass. With these caveats in mind, we take the census time to be 355 days into the reproductive cycle and assume the final weight of the ovaries equals that of eggs. Then, with the reserve turnover rate from the main data set, the models overestimate the reproductive effort in data set SD1 by about a third (see Table 3). With the general reserve turnover rate adjusted (see above), this overestimation increases to 45-70%, though the gonadosomatic index (GSI) remains relatively unaffected as body masses are also predicted higher. Relative to data set SD2, the models underestimate reproduction 25-30%, assuming general reserve turnover rates estimated from the main data set. With those estimates adjusted as before, underestimates shrink to 2% and

20% for dDEB and stdDEB+, respectively, while predicted GSI values change relatively little. The models predict reproductive effort at day 355 as a function of total body mass about similarly, considering the scatter in the data (see Fig. 3B). With general reserve turnover rates adjusted, the measured mean mass and diameter of single eggs in data set SD2, 105.7 (±14.5) mg and 5.54 (±0.36) mm, respectively, are close to the values predicted by dDEB (93.3 mg and 5.62 mm, respectively), whereas the predictions by stdDEB+ differ more (65.3 mg and 4.96 mm, respectively).

Discussion

We have formulated and evaluated two models of feedback control on the production of reproductive matter. The models provide a key to quantitatively connecting molecular level processes to organismal performance, a major challenge in biology. In particular, they describe growth and reproduction as processes subject to hormonal regulation, and thus provide a link between detailed physiologically-based models about the endocrine system (see e.g. Gillies *et al.* 2016) to the DEB modeling framework.

Important strengths of DEB include its generality and relative simplicity. The core dynamics of the standard DEB model for a healthy animal consist of only three state equations and involve universal processes, such as feeding, maintenance, development, reproduction and growth, with similarly general formulae relating these processes to measurable rates, such as respiration, waste and heat production. The additional equations required for modeling particular species and context specific measurable quantities (e.g., Equations 8-19 in Table 1) are somewhat narrower in applicability, but still have considerable generality. For example, we would expect these equations to be applicable to most fishes, albeit with species-specific values for their parameters.

Our representation of demand-driven energy allocation to the production of reproductive matter focuses on a general dynamic mechanism, namely feedback control of gonads. We used this mechanism to develop two extensions of the standard DEB model, stdDEB+ and dDEB (see Figure 1). These extensions share the feature that, depending on the nutritional state of an adult, growth may occur concurrently with the accumulation of reproductive matter; this contrasts with other simple models, often used in optimality arguments, in which an adult commits either resources to growth or to reproduction at any given time (see e.g. Cohen 1971; Quince *et al.* 2008). However, a dDEB organism may cease to grow, and may even shrink, while it continues to allocate resources to reproduction (see below). We evaluated these extensions in depth with data on a single fish species, i.e., rainbow trout, due to the availability of extensive, time-resolved information on whole organism performance as well as on suborganismal processes related to the endocrine system.

Our models describe the production of biomass and reproductive matter in female rainbow trout in the three data sets analyzed here about equally well (see Fig. 2A-D, 3 and Table 3). Values of the core DEB parameter quantifying the rate of general reserve turnover estimated from these data sets differ 20-35% from each other, and they are 10-55% higher than the value published in the DEB parameter database (Kooijman *et al.* 2017), though are rather similar in dDEB and stdDEB+ (see Table 2d). Rainbow trout are a remarkably adaptable species with a long history of domestication and wide geographic distribution, existing as both anadromous and land locked varieties and have a relatively high level of genetic variation among different populations (Maccrimmon 1971; Hershberger 1992). Thus, it is not surprising that the general reserve turnover rate parameter varies among strains. The dDEB variant performs better in describing the dynamics of plasma estradiol and vitellogenin contents as well as the development of individual

391 eggs (see Fig. 2E-G), and overall dDEB fits the main data set significantly better than stdDEB+,
392 as judged from likelihood values (see Table 3). While the types of data best described by dDEB
393 are of relatively minor importance to whole organism performance, their consideration reflects
394 conceptual differences between model variants with important implications.
395 The major conceptual difference between dDEB and stdDEB+ lies in the timing of (somatic)
396 reserve allocation to reproduction. In stdDEB+, a well-fed adult allocates a constant fraction of
397 mobilized reserves to reproduction plus maturity maintenance throughout the reproductive cycle
398 and grows at a rate that is independent of the size of the reproductive buffer. This contrasts with
399 the dynamic allocation of reserves in dDEB, in which the allocation is under the control of the
400 size of the reproductive buffer relative to that of the animal. Consequently, this allocation can
401 vary a great deal over a reproductive cycle (see Fig. S1 in the Supporting Information).
402 Concurrently, growth follows an opposite trend. In a constant environment, dDEB predicts that
403 most of the growth of a species with a seasonal reproduction pattern occurs before the gonads
404 start developing substantially, whereas growth in stdDEB+ is of the von Bertalanffy type.
405 Consequently, size data could discriminate between the two models. Unfortunately, the total
406 body weight measurements analyzed in this study contain too much scatter to be of much help.
407 Length measures typically are relatively precise and could therefore be used to evaluate the
408 merits of dDEB and stdDEB+. It should be noted, though, that dDEB reduces to stdDEB in a
409 hypothetical adult animal that releases gametes nearly continuously, as the density of the
410 reproductive buffer would be almost constant.
411 Both dDEB and stdDEB+ predict the growth of the gonads occurs primarily during the later parts
412 of the reproductive cycle, which is a common observation for synchronous annually spawning
413 fishes like rainbow trout (Tyler & Sumpter 1996) as well as many marine invertebrates,

414 notwithstanding the time-invariant fraction of reserves being allocated to reproduction in the
415 latter model variant. In stdDEB+, this is made possible by separating the reproductive buffer into
416 two sequential pools, of which the first, reproductive reserves, receives somatic reserves
417 according to the kappa rule of standard DEB, whereas the second containing actual reproductive
418 matter (e.g., eggs) exerts positive and negative feedback control on the rate at which it is being
419 filled with reserves from the first pool (see Equations 10-11 and Fig. 1). A potentially unrealistic
420 consequence of separating the reproductive buffer into two pools is that although the gonad pool
421 may be completely emptied during spawning, an animal following stdDEB+ may be left with a
422 substantial amount of reproductive reserves at the time of spawning. Indeed, in stdDEB+
423 parameterized with the main data set, a three year old female rainbow trout releases only a little
424 over 50% of the total amount of somatic reserves allocated to reproduction at spawning, despite
425 its negligible reproductive buffer at the beginning of the reproductive cycle (see Figure S2 in the
426 Supporting Information). In addition, stdDEB+ recognizes two reserve pools, reproductive and
427 somatic, with different dynamics; this begs the question how an animal following stdDEB+
428 would be able to tell apart those reserve pools, given their likely large overlap in chemical nature
429 and storage location.
430 A particular characteristic of dDEB is that reproduction can induce starvation symptoms, even
431 when environmental resources are abundant. Due to the demand driven positive feedback of the
432 reproductive buffer on reserve allocation in dDEB, the energy flow to the somatic branch may
433 become insufficient to meet somatic maintenance demands. At that point, an organism has
434 several options (Kooijman 2010). For instance, it could increase the reserve mobilization rate,
435 give maintenance requirements priority over reproduction, reabsorb reproductive matter, skimp
436 on maintenance, or use structural biomass as an energy source to meet maintenance, i.e., shrink.

All these options may be realistic, depending on the life history strategy of the organism. For instance, reabsorption of gonads under stress conditions occurs in parasitoid wasps (Richard & Casas 2009; Richard & Casas 2012), bivalves (Gosling 2003) and fishes (Schreck, Contreras-Sanchez & Fitzpatrick 2001), among other groups. Here we allowed structural biomass to be recycled for maintenance purposes, but did so in a provisional manner (the thermodynamic implications of shrinking are rather intricate and fall beyond the scope of this paper). This mechanism of structure recycling may be of use to describe the degeneration of structures and the loss in vitality before and after spawning in semelparous fishes, such as species of eel and salmon.

In addition, this recycling mechanism is relevant for species with marked biomass turnover processes, such as holometabolous insects and annual plants. In the pupa stage, holometabolous insects degrade most tissues and build new structures. Without demand-driven feedback mechanisms and implied recycling mechanisms for structural biomass, such as in dDEB, the modeling of holometabolous insects within a DEB context is cumbersome (Llandres *et al.* 2015). Many annual plants feature strategies in which vegetative structures wither while seed mass is still increasing. The common bean, *P. vulgaris*, for instance, clearly displays this pattern (see e.g. Lima *et al.* 2005). In order to illustrate the ability of dDEB to capture this pattern, we used a stripped-down dDEB model without reserves, added an empirical relationship describing the dynamics of relative leaf cover (see Figure 4A) and a simple standard model describing photosynthesis as a function of leaf cover (see Supplemental Information for a full description of the model). This modified dDEB model describes the dynamic allocation of resources to above ground vegetative biomass and reproductive matter in this particular data set quite well (see Fig. 4B). It should be noted that the apparent relocation of structural biomass to seeds is due to an

460 indirect mechanism: structural biomass is metabolized to meet the maintenance demands of the
461 remaining structure, while an increasing fraction of photosynthate is invested in seed production.
462 Our models are designed to serve as pivots connecting Adverse Outcome Pathways (AOP) for
463 endocrine disruptors to processes at ecological levels of organization. AOPs conceptualize the
464 transfer of information from molecular to organismal levels of organization as the first step in
465 scaling up to inform ecological risk assessment (Ankley *et al.* 2010). Starting with one or more
466 molecular initiating events, i.e., perturbations caused by a chemical stressor, AOP models
467 quantify the impacts of that stressor on molecular, cellular and/or organ-level processes.
468 However, these models currently lack the ability to further these impacts to projections of those
469 adverse effects on individual growth, reproduction, and survival, which are in the realm of the
470 DEB modeling framework. Thus, the AOP framework could provide the mechanistic basis for
471 modeling toxic effects within the DEB modeling framework, and thereby opening the door to
472 process-based risk assessments in ecotoxicology (Murphy *et al.* 2018).
473 In conclusion, by including gonadal feedback control on energy allocation to reproduction and
474 somatic processes we obtain three major benefits. Firstly, through this mechanism, the formation
475 of reproductive matter can take on a marked seasonal, semelparous or batch-mode pattern with a
476 minimum of mathematical complexity. Secondly, it facilitates the modeling of growth and
477 reproduction as processes subjected to endocrine regulation, that is, it enables a connection
478 between organismal and suborganismal level processes. Thirdly, since the control variable, i.e.,
479 the density of reproductive matter, has a generic form, species and sex specific attributes of
480 endocrine regulation can be added without changing the core of the model. We anticipate that
481 this mechanism, and our two model extensions that follow from it, will provide a gateway for

incorporating molecular-level mechanisms of endocrine disruption into organismal-level models of individual performance, such as those in the DEB framework.

Authors' contributions

All authors conceived the ideas. EM, KL and RN developed the models. IS collected the data. EM analyzed models and data and led the writing of the manuscript. All authors contributed critically to the drafts and gave final approval for publication.

Data accessibility

Data available from the Dryad Digital Repository: https://doi.org/10.5061/dryad.58j9r88 (Muller *et al.* 2018).

Acknowledgments

We thank Louise Stevenson, Phillipp Antczak, Natàlia Garcia-Reyero, Teresa Mathews, Christopher Remien, Tin Klanjšček and two anonymous reviewers for critical comments. The U.S. Environmental Protection Agency's Science to Achieve Results program supported this work via grants R835797, R835798 and R835167. Partial support was provided by the University of Tours through a visiting fellowship awarded to EM. This work was conducted as a part of the Modeling Molecules-to-Organisms Working Group at the National Institute for Mathematical and Biological Synthesis, sponsored by the National Science Foundation through NSF Award #DBI-1300426, with additional support from The University of Tennessee, Knoxville. This work has not been formally reviewed by EPA or NSF. Any opinions, findings, and conclusions or recommendations expressed in this material are those of the authors and

neither necessarily reflect the views of NSF nor those of EPA. The authors declare no conflicts of interest.

References

AmP (2018) Online database of DEB parameters, implied properties and referenced underlying data. Accessed 2018/09/11. http://www.bio.vu.nl/thb/deb/deblab/add_my_pet/.

Ankley, G.T., Bennett, R.S., Erickson, R.J., Hoff, D.J., Hornung, M.W., Johnson, R.D., Mount, D.R., Nichols, J.W., Russom, C.L., Schmieder, P.K., Serrrano, J.A., Tietge, J.E. & Villeneuve, D.L. (2010) Adverse outcome pathways: a conceptual framework to support ecotoxicology research and risk assessment. *Environmental Toxicology and Chemistry,* **29,** 730-741.

Augustine, S., Gagnaire, B., Adam-Guillermin, C. & Kooijman, S. (2012) Effects of uranium on the metabolism of zebrafish, Danio rerio. *Aquatic Toxicology,* **118,** 9-26.

Brill, R.W., Cousins, K.L., Jones, D.R., Bushnell, P.G. & Steffensen, J.F. (1998) Blood volume, plasma volume and circulation time in a high-energy-demand teleost, the yellowfin tuna (Thunnus albacares). *Journal of Experimental Biology,* **201,** 647-654.

Cohen, D. (1971) Maximizing final yield when growth is limited by time or by limiting resources. . *Journal of Theoretical Biology,* **33,** 299-307.

Einarsson, B., Birnir, B. & Sigurosson, S. (2011) A dynamic energy budget (DEB) model for the energy usage and reproduction of the Icelandic capelin (Mallotus villosus). *Journal of Theoretical Biology,* **281,** 1-8.

Gergs, A. & Jager, T. (2014) Body size-mediated starvation resistance in an insect predator. *Journal of Animal Ecology,* **83,** 758-768.

Gergs, A., Preuss, T.G. & Palmqvist, A. (2014) Double Trouble at High Density: Cross-Level Test of Resource-Related Adaptive Plasticity and Crowding-Related Fitness. *Plos One,* **9**.

Gillies, K., Krone, S.M., Nagler, J.J. & Schultz, I.R. (2016) A Computational Model of the Rainbow Trout Hypothalamus-Pituitary-Ovary-Liver Axis. *Plos Computational Biology,* **12**.

Gosling, E. (2003) *Bivalve molluscs: biology, ecology and culture*. Blackwell.

Hershberger, W.K. (1992) Genetic-variability in rainbow-trout populations. *Aquaculture,* **100,** 51-71.

Jager, T., Barsi, A., Hamda, N.T., Martin, B.T., Zimmer, E.I. & Ducrot, V. (2014) Dynamic energy budgets in population ecotoxicology: Applications and outlook. *Ecological Modelling,* **280,** 140-147.

Jager, T., Ravagnan, E. & Dupont, S. (2016) Near-future ocean acidification impacts maintenance costs in sea-urchin larvae: Identification of stress factors and tipping points using a DEB modelling approach. *Journal of Experimental Marine Biology and Ecology,* **474,** 11-17.

Jusup, M., Sousa, T., Domingos, T., Labinac, V., Marn, N., Wang, Z. & Klanjscek, T. (2017) Physics of metabolic organization. *Physics of Life Reviews,* **20,** 1-39.

Kooijman, S.A.L.M. (1986) Energy Budgets Can Explain Body Size Relations. *Journal of Theoretical Biology,* **121,** 269-282.

Kooijman, S.A.L.M. (2010) *Dynamic energy and mass budgets in biological systems,* 3rd edn. Cambridge University Press, Cambridge.

Kooijman, S.A.L.M., Augustine, S., Sadoul, B. & Zimmer, E.I. (2017) *AmP* Oncorhynchus mykiss, version 2017/05/27. Online database of DEB parameters, implied properties and referenced underlying data, http://www.bio.vu.nl/thb/deb/deblab/add_my_pet/.

Kooijman, S.A.L.M. & Bedaux, J.J.M. (1996) Analysis of toxicity tests on Daphnia survival and reproduction. *Water Research,* **30,** 1711-1723.

Kooijman, S.A.L.M. & Troost, T.A. (2007) Quantitative steps in the evolution of metabolic organisation as specified by the Dynamic Energy Budget theory. *Biological Reviews,* **82,** 113-142.

Lima, E.R., Santiago, A.S., Araujo, A.P. & Teixeira, M.G. (2005) Effects of the size of sown seed on growth and yield of common bean cultivars of different seed sizes. *Brazilian Journal of Plant Physiology,* **17,** 273-281.

Llandres, A.L., Marques, G.M., Maino, J.L., Kooijman, S., Kearney, M.R. & Casas, J. (2015) A dynamic energy budget for the whole life-cycle of holometabolous insects. *Ecological Monographs,* **85,** 353-371.

Maccrimmon, H.R. (1971) World distribution of rainbow trout (*Salmo gairdneri) Journal of the Fisheries Research Board of Canada,* **28,** 663-+.

Muller, E.B., Hanna, S.K., Lenihan, H.S., Miller, R. & Nisbet, R.M. (2014) Impact of engineered zinc oxide nanoparticles on the energy budgets of Mytilus galloprovincialis. *Journal of Sea Research,* **94,** 29-36.

Muller, E.B., Lika, K., Nisbet, R.M., Schultz, I.R., Casas, J., Gergs, A., Murphy, C.A., Nacci, D. & Watanabe, K.H. (2018) Data from: Regulation of reproductive processes with dynamic energy budgets. *Dryad Digital Repository,* https://doi.org/10.5061/dryad.58j9r88.

Muller, E.B. & Nisbet, R.M. (2014) Dynamic energy budget modeling reveals the potential of future growth and calcification for the coccolithophore Emiliania huxleyi in an acidified ocean. *Global Change Biology,* **20,** 2031-2038.

Murphy, C.A., Nisbet, R.M., Antczak, P., Garcia-Reyero, N., Gergs, A., Lika, K., Mathews, T., Muller, E.B., Nacci, D., Peace, A., Remien, C.H., Schultz, I.R., Stevenson, L.M. & Watanabe, K.H. (2018) Incorporating Suborganismal Processes into Dynamic Energy Budget Models for Ecological Risk Assessment. *Integrated Environmental Assessment and Management,* **14,** 615-624.

Nagler, J.J., Cavileer, T.D., Verducci, J.S., Schultz, I.R., Hook, S.E. & Hayton, W.L. (2012) Estrogen receptor mRNA expression patterns in the liver and ovary of female rainbow trout over a complete reproductive cycle. *General and Comparative Endocrinology,* **178,** 556-561.

Nisbet, R.M., Muller, E.B., Lika, K. & Kooijman, S. (2000) From molecules to ecosystems through dynamic energy budget models. *Journal of Animal Ecology,* **69,** 913-926.

Pecquerie, L., Petitgas, P. & Kooijman, S. (2009) Modeling fish growth and reproduction in the context of the Dynamic Energy Budget theory to predict environmental impact on anchovy spawning duration. *Journal of Sea Research,* **62,** 93-105.

Quince, C., Abrams, P.A., Shuter, B.J. & Lester, N.P. (2008) Biphasic growth in fish I: Theoretical foundations. *Journal of Theoretical Biology,* **254,** 197-206.

Richard, R. & Casas, J. (2009) Stochasticity and controllability of nutrient sources in foraging: host-feeding and egg resorption in parasitoids. *Ecological Monographs,* **79,** 465-483.

590 Richard, R. & Casas, J. (2012) A quantitative framework for ovarian dynamics. *Functional*
591 *Ecology,* **26,** 1399-1408.
592 Sale, P.J.M. (1975) Productivity of Vegetable Crops in a Region of High Solar Input. IV. Field
593 Chamber Measurements on French Beans (Phaseolus vulgaris L.) And Cabbages
594 (Brassica oleracea L.). *Australian Journal of Plant Physiology,* **2,** 461-470.
595 Schreck, C.B., Contreras-Sanchez, W. & Fitzpatrick, M.S. (2001) Effects of stress on fish
596 reproduction, gamete quality, and progeny. *Aquaculture,* **197,** 3-24.
597 Schultz, I.R., Nagler, J.J., Swanson, P., Wunschel, D., Skillman, A.D., Burnett, V., Smith, D. &
598 Barry, R. (2013) Toxicokinetic, Toxicodynamic, and Toxicoproteomic Aspects of Short-
599 term Exposure to Trenbolone in Female Fish. *Toxicological Sciences,* **136,** 413-429.
600 Shcherbakov, M.V., Shcherbakova, N.L., Janovsky, T.A. & Kamaev, V.A. (2013) A survey of
601 forecast measures. *World Applied Sciences Journal,* **24,** 171-176.
602 Sousa, T., Domingos, T. & Kooijman, S.A.L.M. (2008) From empirical patterns to theory: a
603 formal metabolic theory of life. *Philosophical Transactions of the Royal Society B-*
604 *Biological Sciences,* **363,** 2453-2464.
605 Sousa, T., Domingos, T., Poggiale, J.C. & Kooijman, S. (2010) Dynamic energy budget theory
606 restores coherence in biology Introduction. *Philosophical Transactions of the Royal*
607 *Society B-Biological Sciences,* **365,** 3413-3428.
608 Stearns, S.C. (1992) *The evolution of life histories*. Oxford University Press, New York.
609 Tyler, C.R. & Sumpter, J.P. (1996) Oocyte growth and development in teleosts. *Reviews in Fish*
610 *Biology and Fisheries,* **6,** 287-318.

611

612

613 **Table 1.** Equations.

DEB Model Expressions		
General reserve density (constant food), m_E		
All variants	fm_{Em}	(1)
Fraction mobilized general reserves to reproduction and maturity maintenance, λ		
stdDEB+, stdDEB	$1-\kappa$	(2)
dDEB	$4\lambda_{\mathrm{m}} m_F \left(m_{F\mathrm{m}} - m_F\right) m_{F\mathrm{m}}^{-2}$	(3)
Growth rate, $dM_V/dt = j_V M_V$		
All variants	$\left(\left(1-\lambda\right)k_E S m_E - j_M\right) M_V \left(\left(1-\lambda\right)m_E + y_V^{-1}\right)^{-1}$	(4)
Dynamics of the density of reproductive buffer in between spawning events, dm_F/dt		
dDEB, stdDEB	$y_F\left(\lambda m_E\left(k_E S - j_V\right) - k_J M_{HD} M_V^{-1}\right) - j_V m_F$	(5)
Dynamics of the density of reproductive reserves, dm_{RE}/dt		
stdDEB+	$y_{RE}\left(\left(1-\kappa\right)\left(k_E S - j_V\right)m_E - k_J M_{HD} M_V^{-1}\right) - m_{RE}\left(j_V + k_F m_G\left(m_{G\mathrm{m}} - m_G\right)\right)$	(6)
Dynamics of the density of reproductive matter in between spawning events, dm_G/dt		
stdDEB+	$y_G k_{RE} m_{RE} m_G\left(m_{G\mathrm{m}} - m_G\right) - j_V m_G$	(7)
Equations Linking Trout Data to DEB quantities		
Total body wet weight, W_B		
dDEB	$\left(1 + m_E + m_F\right) d_M M_V / d_W$	(8)
stdDEB+	$\left(1 + m_E + m_F + m_G\right) d_M M_V / d_W$	(9)
Ovary wet weight, W_O		
dDEB	$\kappa_{OV} m_F d_M M_V / d_W$	(10)
stdDEB+	$\kappa_{OV} m_G d_M M_V / d_W$	(11)
Liver wet weight, W_L		
dDEB	$\left(p + m_F\right)\left(1-\kappa_{OV}\right) d_M M_V / d_W$	(12)
stdDEB+	$\left(p + m_G\right)\left(1-\kappa_{OV}\right) d_M M_V / d_W$	(13)
Mean follicle diameter, L_F		
dDEB	$\left(6\kappa_{OV} d_M M_V m_F / \pi n d_W\right)^{1/3}$	(14)
stdDEB+	$\left(6\kappa_{OV} d_M M_V m_G / \pi n d_W\right)^{1/3}$	(15)

Plasma estradiol concentration, $E2$

dDEB	$q_1 \lambda$	(16)
stdDEB+	$q_2 m_G \left(m_{G\mathrm{m}} - m_G \right)$	(17)

Plasma vitellogenin concentration, V_T

dDEB	$d_T y_F \left(\lambda m_E \left(k_E S - j_V \right) - k_J M_{HD} M_V^{-1} \right) - \left(k_T + j_V \right) V_T$	(18)
stdDEB+	$d_T k_{RE} m_{RE} m_G \left(m_{G\mathrm{m}} - m_G \right) - \left(k_T + j_V \right) V_T$	(19)

Table 2. Parameters and variables used in the analysis of the main set of rainbow trout data. (a) Dynamic model quantities; (b) Experimental variables; (c) fixed parameters; (d) estimated parameters.

(a) Dynamic model quantities

	Interpretation	**Units**
j_V	Specific growth rate	day^{-1}
m_E	Density of general reserves	-
m_F	Density of reproductive buffer (dDEB)	-
m_G	Density of reproductive matter (stdDEB+)	-
m_{RE}	Density of reproductive reserves (stdDEB+)	-
M_V	Amount of structural biomass	C-mole
S	Surface correction function, $(M_{Vm} / M_V)^{1/3}$	-
λ	Fraction of reserves allocated to reproduction (dDEB)	-

(b) Experimental variables

	Interpretation	**Units**
$E2$	Plasma estradiol content	ng ml^{-1}
L_F	Follicle diameter	mm
W_B	Wet weight total body	kg
W_L	Wet weight liver	g
W_O	Wet weight ovaries	kg
V_T	Plasma vitellogenin content	mg ml^{-1}

(c) Fixed parameters (T=11°C)

	Interpretation	Value	Source
d_M	C-mole to dry weight conversion	24.6 g C-mole^{-1}	AmP*
d_W	Wet weight to dry weight conversion	0.2	AmP
f	Scaled food density	0.9	See text**
j_M	Specific maintenance rate	0.025 day^{-1}	AmP
k_J	Maturity maintenance coefficient	0 day^{-1}	See text
m_{F0}	Initial density of reproductive matter (stdDEB+)	0***	See text
m_{Gm}	Maximum density of reproductive matter (stdDEB+)	6.60	See text
$M_{V\mathrm{m}}$	Maximum structural biomass	1.12 C-mole	AmP
y_F	Conversion efficiency general reserve to reproductive buffer	0.95	AmP
y_G	Conversion efficiency reproductive reserve to gonads (stdDEB+)	1	See text
y_{RE}	Conversion efficiency general to reproductive reserve	0.95	AmP
y_V	Conversion efficiency general reserve to structure	0.88	AmP
κ	Fraction reserves allocated to soma (stdDEB+)	0.56	AmP

* 'Add my Pet' DEB parameter data base (Kooijman *et al.* 2017)

** Parameterization section in Materials and Methods

*** Free parameter in dDEB – see Table 2d

628 (d) Estimated parameters

	Interpretation	dDEB		stdDEB+		Units
		Value	95% CI	Value	95% CI	
d_T	Vitellogenin conversion factor	131.6	71.5-339.3	102.2	56.4-404.7	mg day^{-1}
k_E	General reserve turn-over rate	3.37	2.99-3.71	3.63	3.25-3.99	x 10^{-3} day^{-1}
k_{RE}	Reproductive reserve turn-over rate	NA	NA	1.11	1.00-1.24	x 10^{-3} day^{-1}
k_T	Vitellogenin clearance rate	0.044	0.016-0.142	0.032	0.012-0.166	day^{-1}
m_{F0}	Initial density of reproductive buffer	1.67	0.66-3.64	NA*	NA*	x 10^{-3}
m_{Fm}	Maximum density of reproductive buffer	3.67	3.20-4.21	NA	NA	-
m_{G0}	Initial density of reproductive matter	NA	NA	9.28	4.60-17.5	x 10^{-3}
M_{V0}	Initial amount of structural biomass	0.846	0.787-0.915	0.827	0.770-0.890	C-mole
n	Number of eggs	4.43	3.57-5.48	5.15	4.10-6.52	x 10^3 #
p	Compound parameter, $(\kappa_{VL}+\kappa_{EL}m_E)/(1-\kappa_{OV})$	5.50	3.52-10.89	5.76	3.63-11.6	-
q_1	Estradiol conversion factor	56.0	44.6-66.9	NA	NA	ng ml^{-1}
q_2	Estradiol conversion factor	NA	NA	3.40	2.58-4.24	ng ml^{-1}
V_{T0}	Initial plasma vitellogenin content	102.3	66.1-142.6	96.7	57.2-144.9	mg ml^{-1}
κ_{OV}	Fraction of reproductive matter in ovaries	0.971	0.957-0.984	0.967	0.951-0.982	-
λ_m	Maximum fraction of reserves to reproduction	0.761	0.684-0.839	NA	NA	-

629

630 * Fixed parameter in stdDEB+ - see Table 2c.

631

632 **Table 3.** Statistics of model fits to Main data set[1].

Data type	Figure	dDEB $\ln\mathcal{L}=-1551.2$			stdDEB+ $\ln\mathcal{L}=-1573.1$		
		σ	*SMScE*	*ME*	σ	*SMScE*	*ME*
$E2$	2G	11.8 ng. ml^{-1}	0.592	0.556	14.2 ng ml^{-1}	0.724	0.363
L_F	2E	0.445 mm	0.162	0.906	0.491 mm	0.298	0.885
W_B	2A	170 g	0.077	0.811	157 g	0.071	0.838
W_L	2D	5.66 g	0.176	0.449	5.70 g	0.175	0.439
W_O	2B	44.7 g	0.304	0.871	47.7 g	0.298	0.853
$W_B - W_O$	2C	305 g	0.109	0.071	299 g	0.107	0.110
V_T	2F	35.2 mg ml^{-1}	0.542	0.644	40.3 mg ml^{-1}	0.635	0.534
Overall	2		0.280	0.615		0.309	0.575

633 [1]A perfect fit implies $SMScE=0$ and $ME=1$.

634

635 **Table 3.** Measured and predicted body and egg masses supplementary data sets on day 355.

Set		Body mass	Egg mass	GSI
SD1	Data	2608 (±393)	274 (±84)	0.105
	dDEB, k_E from main set	2096 (±188)	373 (±34)	0.178
	dDEB, k_E 25% higher	2660 (±220)	470 (±40)	0.177
	stdDEB, k_E from main set	2177 (±197)	370 (±42)	0.170
	stdDEB, k_E 20% higher	2629 (±223)	400 (±46)	0.152
SD2	Data	2483 (±663)	419 (±161)	0.169
	dDEB, k_E from main set	1732 (±201)	296 (±35)	0.171
	dDEB, k_E 35% higher	2428 (±251)	412 (±43)	0.170
	stdDEB, k_E from main set	1849 (±213)	308 (±67)	0.167
	stdDEB, k_E 20% higher	2263 (±246)	336 (±80)	0.149

636

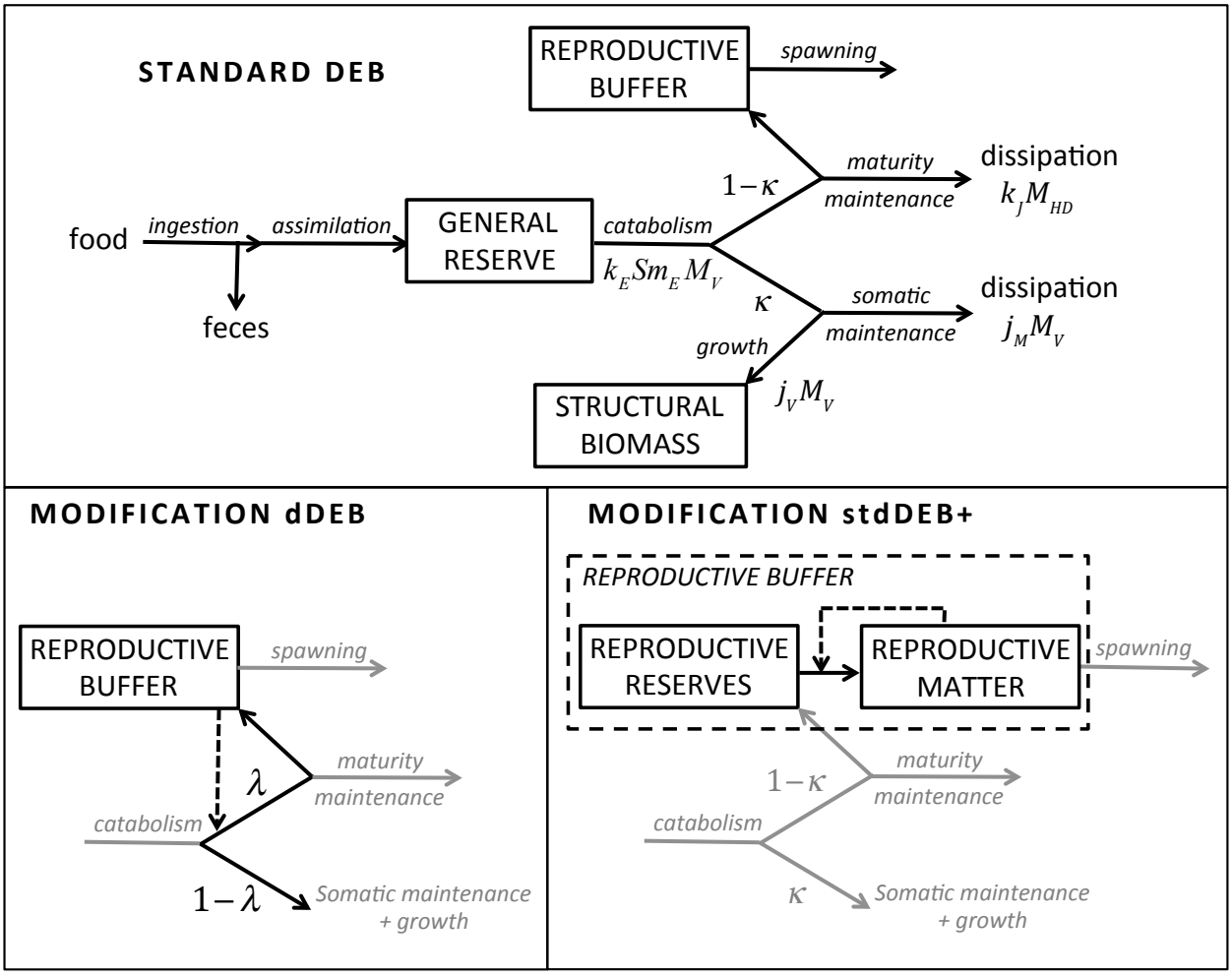

Figure 1. Conceptual representations of the standard DEB (stdDEB) model for healthy adults and of two types of modifications, dDEB and stdDEB+. stdDEB (Nisbet *et al.* 2000; Kooijman 2010; Jusup *et al.* 2017) describes the rates at which an adult animal acquires food, assimilates the energy and nutrients therein into general reserves, and allocates those reserves to somatic and maturity maintenance, growth and reproduction; this allocation is defined as catabolism. A fixed fraction κ of the catabolic flux is allocated to somatic maintenance and growth. Somatic and maturity maintenance are demand-driven processes and take priority over growth and reproduction; all other processes in stdDEB are supply-driven. In dDEB, stdDEB is modified to include positive and negative feedback of the reproductive buffer on the allocation of the catabolic flux. Thus, in dDEB, reproduction is a demand-driven process with a variable fraction λ of the catabolic flux allocated to maturity maintenance and reproduction. stdDEB+ separates the reproductive buffer in two pools: reproductive reserves and actual reproductive matter (gonads). The rate at which reproductive reserves are converted into reproductive matter depends on the densities of reproductive reserve and reproductive matter, implying that gonad loading is a demand-driven process. Solid arrows represent energy and material fluxes; broken arrows

represent feedback mechanisms; boxes represent state variables; modifications of dDEB and stdDEB+ relative to stdDEB are presented in black while communalities are shown in grey. Note that DEB processes and quantities are abstractions; auxiliary rules are required to relate them to experimental quantities – see Table 1.

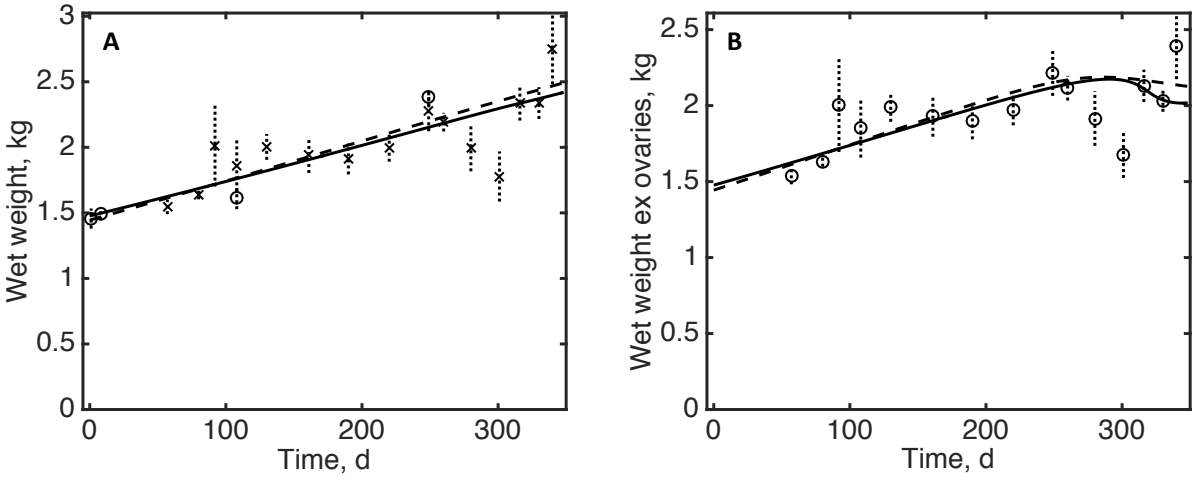
A
Wet weight, kg
Time, d
B
Wet weight ex ovaries, kg
Time, d

659

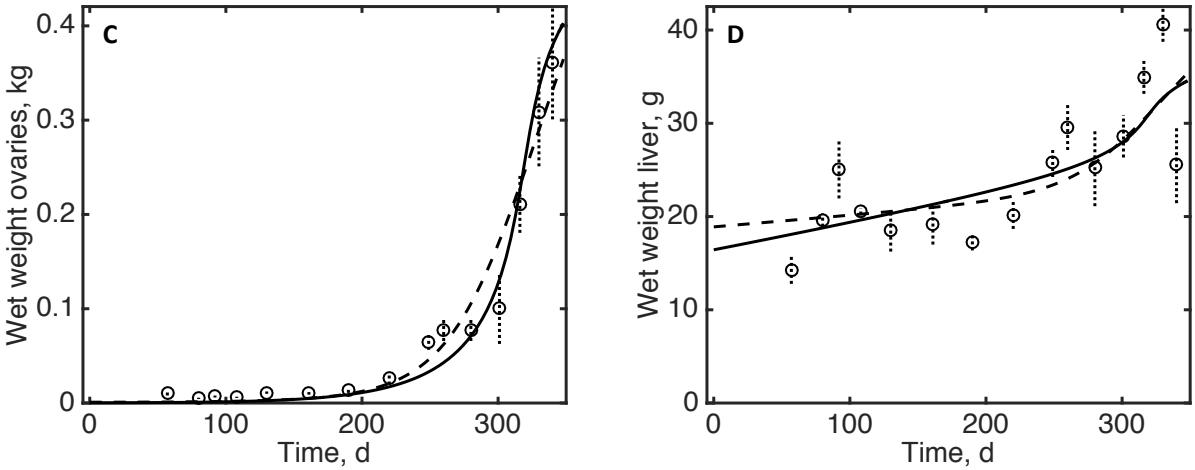
C
Wet weight ovaries, kg
Time, d
D
Wet weight liver, g
Time, d

660

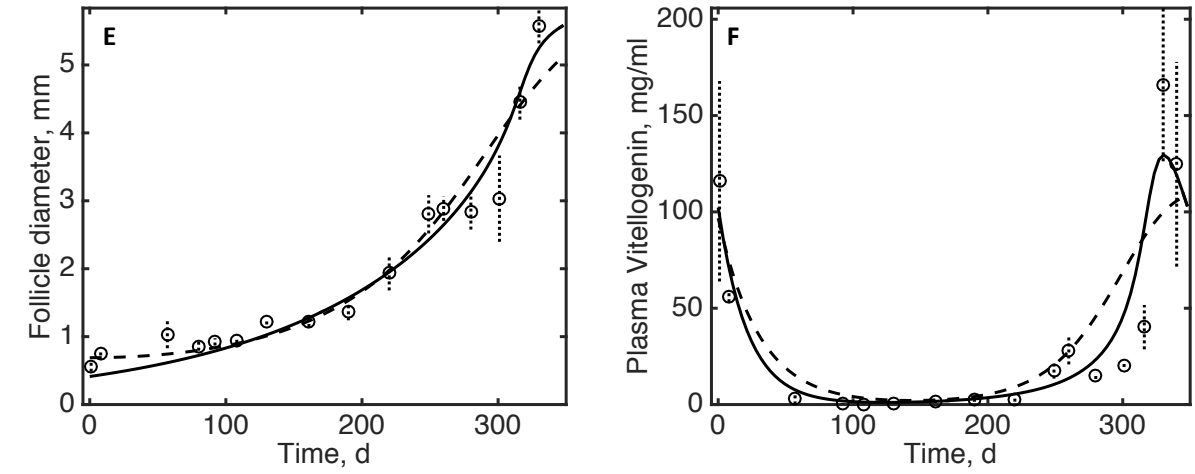
E
Follicle diameter, mm
Time, d
F
Plasma Vitellogenin, mg/ml
Time, d

661

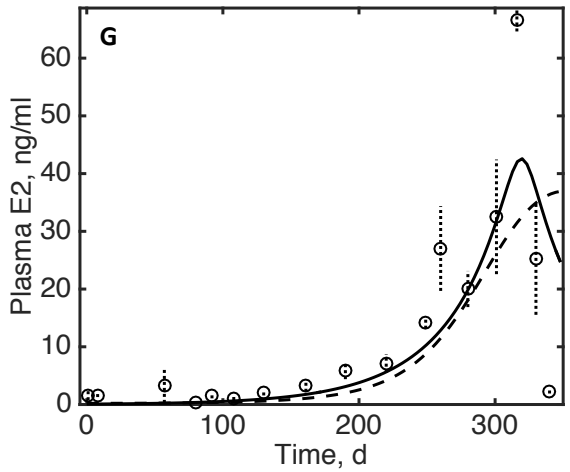

662

663 **Figure 2.** Model fits of dDEB (solid line) and stdDEB+ (dashed line) to main data set with
664 rainbow trout (symbols), including (A) total body wet weight; (B) total body wet weight less wet
665 weight of ovaries; (C) wet weight of ovaries; (D) wet weight of liver; (E) mean diameter of
666 maturing follicles (mean per fish); (F) plasma vitellogenin content; and (G) plasma estradiol
667 content. Measurements denoted 'x' in Panel A were used to calculate corresponding data in
668 Panel B and were therefore omitted in the fitting procedure. Error bars denote standard
669 deviations (n = 3 or 4). Parameter estimates are given in Table 1d and goodness-of-fit measures
670 in Table 2. Data from Nagler *et al.* (2012) and Gillies *et al.* (2016).

671

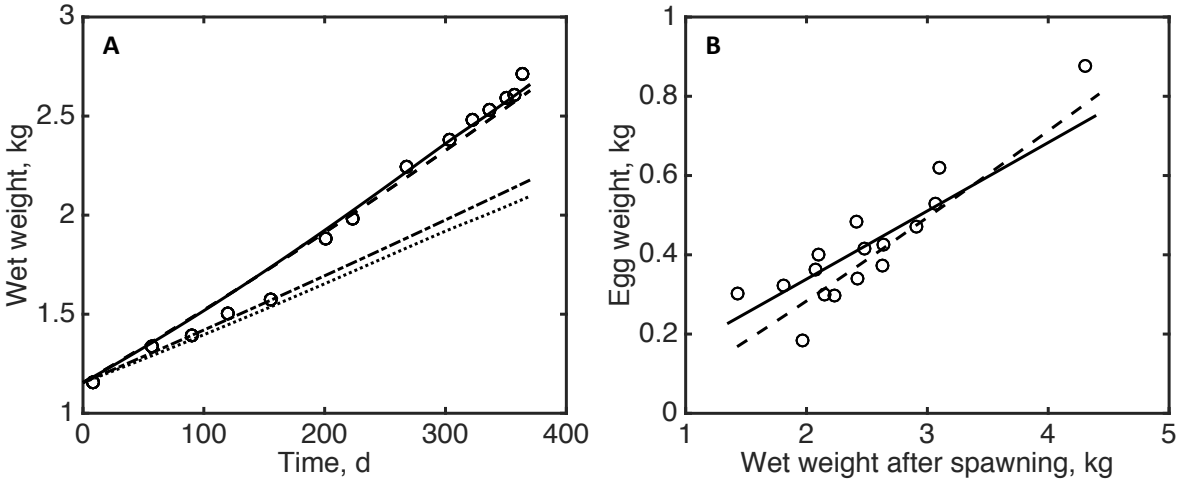

Figure 3. The ability of dDEB and stdDEB+ parameterized with values estimated from the main data set (see Fig. 2 and Table 1d) to predict production in rainbow trout was evaluated with supplementary data set SD1 (A) and set SD2 (B). (A) With the estimated parameter values, both dDEB (dotted curve) and stdDEB+ (dot-dashed curve) underestimated the gain in weight in set SD1 (circles). Predictions are greatly improved by increasing the reserve turnover rate by 25% (dDEB, solid curve) or 20% (stdDEB+, broken curve) relative to the value estimated from the main data set. (B) dDEB (solid curve, reserve turnover rate 35% higher than the one in the main data set) and stdDEB+ (broken curve, reserve turnover rate 20% higher than the one in the main set) predict measured total egg mass versus body weight (symbols) from data set SD2 about equally well.

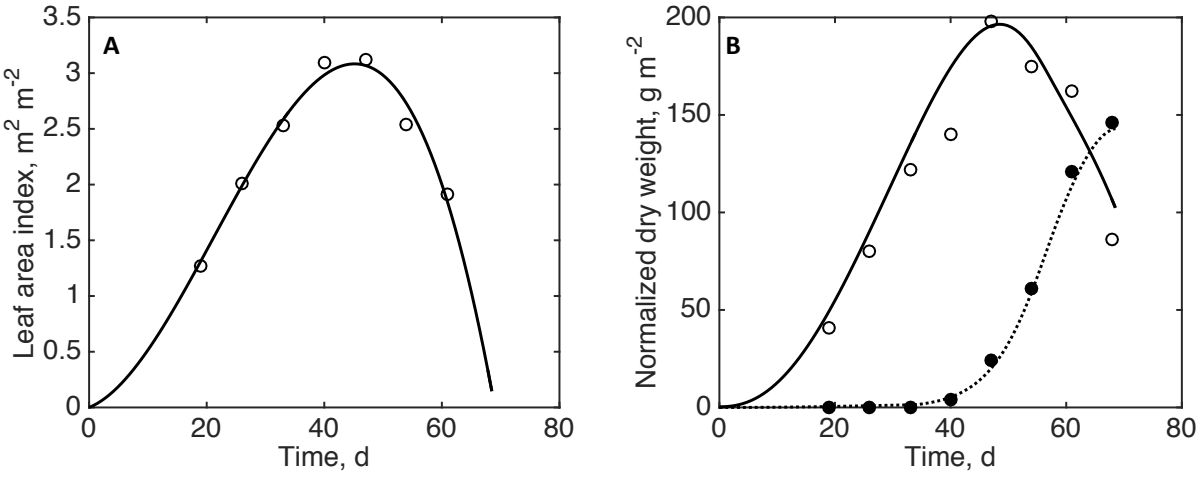

686

687

688 **Figure 4.** Application of a simplified version of dDEB to production in the common bean,
689 *Phaseolis vulgaris*. (A) An empirical third degree polynomial describes the dynamics of the leaf
690 area index, defined as the total green leaf surface are per unit area ground cover, an important
691 determinant of the photosynthetic capacity ($p_1 = 30.5\ \mathrm{min}^{-1}$, $p_2 = 5.2\ \mathrm{min}^{-2}$, $p_3 = -0.08\ \mathrm{min}^{-3}$).
692 (B) The simplified dDEB model fits above ground vegetative biomass (open circles, solid curve)
693 and pod mass (closed circles, dotted curve) with mean bean mass as the initial amount of
694 structural biomass, observed mean time of first flowering (34 d) as starting point of
695 photosynthate allocation to reproduction, $m_F = 0.01$ and negligible losses in converting
696 photosynthate into vegetative and reproductive biomass. Parameter estimates (with 95%
697 confidence intervals) are $\lambda_m =$ 0.52 (0.30-0.87), $m_{Fm} =$ 1.09 (0.95-1.24), $j_M =$ 0.08 (0.03-0.16)
698 d^{-1} and $c =$ 0.12 (0.08-0.17); $J^{\circ}_{Pm} =$ 65.2 g dry weight m^{-2} d^{-1}- based on the net photosynthesis
699 rate estimated by Sale (1975). Data are from Lima *et al.* (2005) and represent the means of four
700 replicates of six cultivars grown from large seeds. See Supplemental Information for model
701 description.

SUPPORTING INFORMATION - REGULATION OF REPRODUCTIVE PROCESSES WITH DYNAMIC ENERGY BUDGETS

Erik B. Muller[1,2*], Konstadia Lika[3], Roger M. Nisbet[4], Irvin R. Schultz[5], Jérôme Casas[6], André Gergs[7,8], Cheryl A. Murphy[9], Diane Nacci[10], Karen H. Watanabe[11]

[1]Department of Biology. Norwegian University of Science and Technology, Trondheim, Norway

[2]Marine Science Institute, University of California, Santa Barbara, CA, USA

[3]Department of Biology, University of Crete, Heraklion, Greece

[4]Department of Ecology, Evolution and Marine Biology, University of California, Santa Barbara, CA, USA

[5]Pacific Northwest National Laboratory, Marine Sciences Laboratory, Sequim, WA, USA.
Current Address: Lynker Technologies under contract to Northwest Fisheries Science Center, National Marine Fisheries Service, National Oceanic and Atmospheric Administration, Seattle, WA, USA.

[6]Institute de Recherche sur la Biologie de l'Insecte, Université de Tours, Tours, France

[7]gaiac - Research Institute for Ecosystem Analysis and Assessment, Aachen, Germany

[8]current affiliation: Bayer AG, Monheim, Germany

[9]Department of Fisheries and Wildlife, Michigan State University, East Lansing, MI, USA

[10]US Environmental Protection Agency, Office of Research and Development, Narragansett, RI, USA

[11]School of Mathematical and Natural Sciences, Arizona State University, Glendale, AZ, USA

[*]Corresponding author erik.muller@lifesci.ucsb.edu , bpbleus@yahoo.com

TROUT CULTIVATION

All trout were maintained according to the guidelines established by the Institutional Animal Care and Use Committee (IACUC) of Battelle PNNL. Adult female rainbow trout were

purchased from a local trout hatchery (Nisqually trout farm, Lacey, WA USA http://nisquallytrout.com/ntfwebsite_001.htm) 7-days after completing their first spawning cycle. After transfer to the Battelle Marine Sciences Laboratory (MSL; Sequim, WA USA), trout were initially placed in circular, 1400L fiberglass tanks, maintained as a single pass flow-through freshwater system with water in-flow rates set to 15-20 L / min. The source water was from Battelle MSL's artesian well (well depth = 134 m). Several 6" ceramic air diffusers were added to each tank to maintain oxygen saturation. One week after arrival at MSL (14 days post-spawn), trout were weighed and tagged with passive inducible transponders (Biomark HPT8, Biomark Inc, Boise ID USA) to permit identification. After tagging, groups of five trout were housed in 370 L fiberglass tanks with water in-flow rates set to 4-5 L/min. Selected water quality parameters routinely measured in all tanks were: temperature (mean 11.6 ^{o}C; range: 9.8 – 13.1 ^{o}C), dissolved oxygen (mean 9.2; range 8.9 – 10.4 mg/L) and pH (mean 7.9; range: pH 7.8 – 7.95) during the study. Trout were maintained under lighting that simulated the natural photoperiod according to the latitude for Sequim WA, USA (48.079 N) and included a 12-min graded sunrise/sunset period. The larger holding tanks were partially covered with a black tarp to provide shading while the smaller tanks were fitted with a fiberglass lid that permitted diffuse light to enter the tank. Trout were fed daily with a soft moist feed (BioBrood 6 mm pellet; Bio-Oregon Inc, Longview, WA USA http://www.bio-oregon.com/BioBrood-P56.aspx), at a ration level (approximately 1.0 % body mass /d) designed to maximize growth and ovarian maturation during the study.

MODEL DERIVATIONS

The standard model of Dynamic Energy Budget (stdDEB) theory (see Fig. 1 in the main text) describes the rates at which a 'generalized' animal acquires resources from its environment and uses the energy therein for somatic and maturity maintenance, growth, maturation (juveniles) and reproduction (adults). A 'generalized' animal is heterotrophic, grows isometrically (constant shape), does not encounter conditions of stress (including debilitating forms of starvation), and has three life stages: embryonic (during which it does not feed), juvenile (feeding but no reproduction) and adult. This study only considers the adult stage. Kooijman (2010) has described this theory and its standard formulation in detail and several other publications provide

extensive summaries (Nisbet *et al.* 2000; Sousa, Domingos & Kooijman 2008; Jusup *et al.* 2017).

DEB models can be cast in terms of size, energy and/or mass units. Unit choice is largely a matter of convenience due to the existence of conversion rules. Here we use mass as the primary unit. To avoid the introduction of parameters with fractional powers of mass as part of their units, we use a surface correction function, *S*,

$$S = \left(\frac{M_{V\mathrm{m}}}{M_V} \right)^{1/3} \tag{S1}$$

in which M_V is the amount of structural biomass and $M_{V\mathrm{m}}$ the maximum amount of structural biomass an animal would ultimately attain at abundant food conditions (based on its bioenergetic parameters in the embryo stage). Note that *S* decreases with M_V and thus with time in growing animals.

The standard DEB model (stdDEB) for a 'generalized' adult animal has dynamic equations for the general reserve density, i.e., the ratio of the amount of general reserves (M_E) and structural biomass, $m_E \equiv M_E / M_V$, the amount of structural biomass, and the production of reproductive buffer. The dynamics are

$$\frac{dm_E}{dt} = \left(j_{Am} f - k_E m_E \right) S \tag{S2}$$

$$\frac{dM_V}{dt} = \frac{\kappa k_E S m_E - j_M}{\kappa m_E + y_V^{-1}} M_V = j_V M_V \tag{S3}$$

$$J_F = y_F \left(\left(1 - \kappa \right) m_E M_V \left(k_E S - j_V \right) - k_J M_{HD} \right) \tag{S4}$$

in which j_{Am} is the maximum specific assimilation rate ('specific' means a quantity is scaled to the amount of structural biomass); f is the scaled food density, which takes values between 0 (no food) and 1 (abundant food); k_E is the reserve turn-over rate; j_M and j_V are the specific

77 rates of maintenance and growth, respectively; y_V and y_F are the efficiencies with which
78 reserves are converted into structure and material in the reproductive buffer, respectively; and
79 $k_J M_{HD}$ is the rate at which reserves are committed to maintain the attained state of maturity,
80 M_{HD} (this rate is constant in non-starving adults). Note that uppercase '*M*' and '*J*' refer to
81 absolute quantities, whereas their lower case counterparts denote corresponding quantities
82 expressed per unit of structural biomass. Note also that the general reserve density reaches
83 equilibrium at $m_E = j_{Am} f / k_E$ in a constant food environment, and has a maximum when $f = 1$,
84 $m_{Em} \equiv j_{Am} / k_E$.

85 The parameter κ characterizing partitioning of mobilized reserve is constant in stdDEB but is
86 under the control of the reproductive buffer in dDEB. In order to avoid confusion, in the latter
87 variant we use

88 $$\lambda \equiv 1 - \kappa \qquad \text{(S5)}$$

89 In order to specify λ and the dynamics of the density of reproductive matter in the reproductive
90 buffer, m_F, we assume the following for the dDEB model variant:

91 1. At the onset of a reproductive cycle, a small fraction of somatic biomass is converted to
92 reproductive matter, e.g., due to meiosis. General reserves and structure contribute
93 proportionally to the initial formation of reproductive matter, and the costs of this
94 conversion are negligible. The latter two assumptions are rather arbitrary but
95 quantitatively insubstantial.

96 2. The initial density of reproductive matter is constant. This assumption maintains
97 parameter parsimony and model simplicity.

98 3. An adult has a bounded capacity to carry reproductive matter. In non-starving adults, this
99 capacity is proportional to the amount of structural biomass, i.e., the maximum density of
100 reproductive matter is a constant. This assumption maintains parameter parsimony and
101 model simplicity.

4. The fraction of mobilized general reserve allocated to reproduction and maturity maintenance in adults is proportional to (1) the density of reproductive matter, and (2) the difference between the maximum and actual density of reproductive matter. The first proportionality introduces positive feedback and is based on the general observation that the ovaries in fish produce estrogen, which stimulates the production of vitellogenin, the precursor of egg reserve material (Tyler & Sumpter 1996). The second proportionality provides a simple negative feedback (i.e., deceleration) mechanism that causes the accumulation of reproductive material in the gonads to slow down towards the end of a reproductive cycle.

5. Spawning requires the density of reproductive matter to exceed a threshold and, additionally, may be under the control of a time trigger or environmental factor, depending on species.

Thus, $\lambda \propto m_F\left(m_{Fm} - m_F\right)$, with m_F and $m_{F\mathrm{m}}$ being the density of reproductive matter and maximum density of reproductive matter, respectively. λ reaches a maximum when $m_F = 0.5m_{F\mathrm{m}}$, so $\lambda_{\mathrm{m}} \propto 0.25m_{F\mathrm{m}}^2$. Accordingly,

$$\lambda = \frac{4\lambda_{\mathrm{m}} m_F\left(m_{F\mathrm{m}} - m_F\right)}{m_{F\mathrm{m}}^2} \tag{S6}$$

with $0 \le \lambda \le \lambda_{\mathrm{m}} \le 1$.

stdDEB+ is a modified version of a capelin model by Einarsson, Birnir and Sigurosson (2011). The reproductive buffer is separated into reproductive reserves and reproductive matter. In order to specify the dynamics of these two reproductive pools, we make assumptions that are analogous to those in dDEB. In particular, we use assumptions 1-3 and 5 from dDEB (but note the difference between the definition of reproductive matter in stdDEB+ (roughly, the contents of gonads) and that in dDEB (all matter earmarked for reproduction)), and make the following additional assumptions:

6. The efficiency with which reproductive reserves are converted into reproductive matter is constant.

7. The rate at which reproductive reserves are converted to reproductive matter is proportional to (1) the density of reproductive reserves, (2) the density of reproductive matter, (3) to the difference between the maximum and actual density of reproductive matter, and (4) the amount of structural biomass. The first proportionality ensures the density of reproductive reserves cannot become negative. Arguments for the two subsequent proportionalities are similar to those given in the fourth assumption of dDEB.

Thus, the production rate of reproductive matter in stdDEB+, J_G, can be expressed as

$$J_G = y_G k_{RE} m_{RE} m_G \left(m_{G\mathrm{m}} - m_G \right) M_V \tag{S7}$$

with y_G as the conversion efficiency of reproductive reserves into reproductive matter; k_{RE} as the reproductive reserves turn-over rate; m_{RE} as the density of reproductive reserves; and m_G and $m_{G\mathrm{m}}$ as the density of reproductive matter and maximum density of reproductive matter in stdDEB+, respectively.

We can now summarize the dynamics of the state variables in dDEB and stdDEB+. For both model variants, the reserve density dynamics are given in Equation S2, and Equation S3 describes the growth dynamics in stdDEB+. The growth dynamics in dDEB are obtained by substituting Equation S5 into S3

$$\frac{dM_V}{dt} = \frac{\left(1-\lambda\right) k_E S m_E - j_M}{\left(1-\lambda\right) m_E + y_V^{-1}} M_V = j_V M_V \tag{S8}$$

with λ given in Equation S6.

Similarly, the dynamics of the density of reproductive matter in between spawning events in dDEB follow from Equation S4,

$$\frac{dm_F}{dt} = j_F - j_V m_F = y_F \left(\lambda m_E \left(k_E S - j_V \right) - \frac{k_J M_{HD}}{M_V} \right) - j_V m_F \tag{S9}$$

149 in which $j_F \equiv J_F / M_V$. The last term denotes dilution due to growth, which arises from the chain
150 rule for differentiation and $m_F = M_F / M_V$.

151 In stdDEB+, the dynamics of the densities of reproductive reserves and reproductive matter
152 follow from Equations S4 and S7:

153
$$\begin{aligned}\frac{dm_{RE}}{dt} &= j_F - j_V m_{RE} - \frac{j_G}{y_G} \\ &= y_{RE}\left((1-\kappa)\left(k_E S - j_V\right) m_E - \frac{k_J M_{HD}}{M_V} \right) - j_V m_{RE} - k_{RE} m_{RE} m_G \left(m_{G\mathrm{m}} - m_G \right)\end{aligned} \tag{S10}$$

154
$$\frac{dm_G}{dt} = j_G - j_V m_G = y_G k_{RE} m_{RE} m_G \left(m_{G\mathrm{m}} - m_G \right) - j_V m_G \tag{S11}$$

155 The dilution terms in Equations 10 and 11 stem from the chain rule for differentiation, as in
156 Equation 9, and $j_G \equiv J_G / M_V$.

157

158 ## LINK BETWEEN DEB QUANTITIES AND DATA

159 Variables in DEB models are abstract quantities and therefore do not correspond directly with
160 measurable quantities. The mapping of DEB quantities onto the data analyzed in this study,
161 including total body, ovary and liver wet weights, follicle diameter and plasma levels of estradiol
162 and vitellogenin, are achieved through auxiliary assumptions stated in this section.

163 In DEB models, the molecular formulae of organic compounds, including the composite biomass
164 compounds in stdDEB+ and dDEB, are reduced to their empirical counterparts and then scaled to
165 contain a single carbon atom. The mass unit is then mole of carbon, or C-mole. In order to
166 convert biomass in structure, reserves and the reproductive buffer to wet weights, we assume that
167 a C-mole of structure, reserves and material in the reproductive buffer have identical dry
168 weights, and that each biomass type has the same water content. Since the total body wet weight,
169 W_B, equals the sum of wet weights of all types of biomass, in dDEB

$$W_B = \left(M_V + M_E + M_F\right) d_M / d_W = \left(1 + m_E + m_F\right) d_M M_V / d_W \quad \text{(S12)}$$

and in stdDEB+,

$$W_B = \left(M_V + M_E + M_{RE} + M_G\right) d_M / d_W = \left(1 + m_E + m_{RE} + m_G\right) d_M M_V / d_W \quad \text{(S13)}$$

in which d_M is the dry weight of a C-mole of biomass and d_W the ratio of the dry weight and wet weight of a unit of biomass; the absolute amounts of matter in the reproductive buffer, M_F, and reproductive reserves, M_{RE}, and actual reproductive matter, M_G, relate to their respective densities through $m_* = M_* / M_V$.

Considering that the ovaries mainly consist of storage materials in eggs, we assume the contributions of structure and general reserves to the wet weight of the ovaries are negligible (to avoid confusion, we will use 'storage' to refer to physical materials and 'reserves' as the conceptual abstraction in the context of DEB). We also assume that the fraction of reproductive matter that is in the ovaries, κ_{OV}, is constant. Then the wet weight of the ovaries, W_O, in dDEB is

$$W_O = \kappa_{OV} m_F d_M M_V / d_W \quad \text{(S14)}$$

and in stdDEB+,

$$W_O = \kappa_{OV} m_G d_M M_V / d_W \quad \text{(S15)}$$

Since the wet weight measurements in the data sets analyzed in this study include only those of the total body, ovaries and liver, we assume that reproductive matter is either in the ovaries or in the liver, which produces the precursors of egg storage materials. We exclude plasma vitellogenin, the precursor of egg storage materials, from reproductive matter for reasons discussed in the main text.

We assume that the fractions of structure and reserves that are part of the liver, κ_{VL} and κ_{EL}, respectively, are constant. Additionally, in order to retain simplicity in stdDEB+, we consider the amount of reproductive reserves in the liver to be negligible. Thus, in dDEB

194 $$W_L = \left(\kappa_{VL} + \kappa_{EL} m_E + \left(1-\kappa_{OV}\right) m_F\right) \frac{d_M M_V}{d_W} = \left(p + m_F\right) \frac{\left(1-\kappa_{OV}\right) d_M M_V}{d_W} \quad \text{(S16)}$$

195 and in stdDEB+

196 $$W_L = \left(\kappa_{VL} + \kappa_{EL} m_E + \left(1-\kappa_{OV}\right) m_G\right) \frac{d_M M_V}{d_W} = \left(p + m_G\right) \frac{\left(1-\kappa_{OV}\right) d_M M_V}{d_W} \quad \text{(S17)}$$

197 in which $p = \left(\kappa_{VL} + \kappa_{EL} m_E\right) / \left(1-\kappa_{OV}\right)$ is a compound parameter in constant food environments.

198 In order to relate the mean diameter of a follicle to reproductive matter, we assume that follicles
199 are perfect spheres and that the specific gravity of biomass equals unity. Accordingly, in dDEB

200 $$L_F = \left(\frac{6\kappa_{OV} d_M M_V m_F}{\pi n d_W} \right)^{1/3} \quad \text{(S18)}$$

201 and in stdDEB+

202 $$L_F = \left(\frac{6\kappa_{OV} d_M M_V m_G}{\pi n d_W} \right)^{1/3} \quad \text{(S19)}$$

203 with n as the number of follicles in the ovaries.

204 Estradiol is produced by the ovaries and regulates the flow of vitellogenin to the ovaries.
205 Accordingly, we link the gonad loading module of stdDEB+ and the reproduction flux in dDEB
206 to the plasma estradiol concentration, $E2$. Considering that proportionality provides the simplest
207 link, we assume for dDEB

208 $$E2 = q_1 \lambda \quad \text{(S20)}$$

209 and for stdDEB+

210 $$E2 = q_2 m_G \left(m_{G\mathrm{m}} - m_G\right) \quad \text{(S21)}$$

211 To model the dynamics of plasma vitellogenin, we assume that the volume of plasma is
212 proportional to the amount of structural biomass, and that the rate at which vitellogenin is cleared

from plasma is proportional to the amount of structural biomass (e.g., by structural mass in the ovaries). Furthermore, for dDEB, we assume that the rate at which vitellogenin is released into the blood stream is proportional to the rate at which somatic reserves are allocated to reproduction. With d_T and k_T as the proportionality density factor converting the density of reserves assigned to reproduction to plasma vitellogenin content, and vitellogenin clearance rate, respectively, the dynamics of plasma vitellogenin content, V_T , are

$$\frac{dV_T}{dt} = d_T j_F - \left(k_T + j_V\right)V_T = d_T y_F \left(\lambda m_E \left(k_E S - j_V\right) - \frac{k_J M_{HD}}{M_V} \right) - \left(k_T + j_V\right)V_T \qquad \text{(S22)}$$

For stdDEB+, we assume that the rate at which vitellogenin is released into the blood stream is proportional to the rate at which reproductive reserves are allocated to reproductive matter, implying

$$\frac{dV_T}{dt} = \frac{d_T j_G}{y_G} - \left(k_T + j_V\right)V_T = d_T k_{RE} m_F^{'} m_G \left(m_{G\mathrm{m}} - m_G\right) - \left(k_T + j_V\right)V_T \qquad \text{(S23)}$$

SIMPLIFIED dDEB MODEL FOR ANNUAL PLANTS

Canopy configuration is an important determinant of the photosynthetic capacity of a plant. A summary statistic for canopy configuration is the Leaf Area Index (LAI), which is defined as the ratio of the area of all green leaves to the ground area under the canopy. A commonly used simple model relating the gross photosynthesis rate per unit ground area, J_P°, to LAI, L, assumes an even leaf distribution, the Lambert-Beer law for incidence light absorption and a linear relationship between light absorption and photosynthesis,

$$J_P^\circ = J_{Pm}^\circ \left(1 - e^{-cL}\right) \qquad \text{(S24)}$$

in which J_{Pm}° is the maximum gross photosynthesis rate (per unit ground area) and c a light absorption coefficient.

In order to retain maximum simplicity, we ignore reserves and assume that photosynthate is used for somatic maintenance and growth until the time first flowers appear, t_D, and partitioned between reproduction and somatic maintenance plus growth as in dDEB, with the caveat that the

fraction of photosynthate allocated to growth cannot exceed λ_m. Thus, with J_F° and M_V° as the reproduction rate and amount of structural biomass, respectively, normalized to ground surface area,

$$\lambda = \begin{cases} \min\left(\lambda_{\mathrm{m}}, \dfrac{4\lambda_{\mathrm{m}} m_F \left(m_{F\mathrm{m}} - m_F\right)}{m_{F\mathrm{m}}^2}\right) & \text{if } t \geq t_D \\ 0 \text{ otherwise} \end{cases} \tag{S25}$$

$$\frac{dM_V^\circ}{dt} = j_V M_V^\circ = y_V \left(1-\lambda\right) J_P^\circ - j_M M_V^\circ \tag{S26}$$

$$\frac{dm_F}{dt} = \frac{J_F^\circ}{M_V^\circ} - j_V m_F = \frac{y_F \lambda J_P^\circ}{M_V^\circ} - j_V m_F \tag{S27}$$

in which j_V and j_M is the specific growth and maintenance rate, respectively (units: time^{-1}). When $y_V\left(1-\lambda\right) < J_P^\circ j_M M_V^\circ$, shrinking occurs.

In our example with common beans, we equate pod mass with reproductive biomass, and take above ground vegetative biomass cover as a proxy for structure. In order to relate LAI to above ground vegetative mass, we describe the dynamics of LAI by fitting a third degree polynomial to LAI data,

$$L = p_3 t^3 + p_2 t^2 + p_1 t \tag{S28}$$

We assume that maximum gross photosynthesis rate equals the maintenance demands of a common bean at its maximum observed size plus its maximum net photosynthesis rate of 40 mg CO_2 dm^{-2} h^{-1} as determined by Sale (1975). Sale's estimate corresponds to about 50 g biomass dry weight m^{-2} d^{-1}, assuming biomass consists of nearly 50% carbon.

GOODNESS-OF-FIT MEASURES

The symmetric mean scaled error, $SMScE_i$, and the model efficiency, ME are calculated with

$$SMScE_i = \frac{2\sum_{j=1}^{n} \left| y_{ij} - y_{ij}^* \right|}{\sum_{j=1}^{n} \left(y_{ij} + y_{ij}^* \right)} \tag{S29}$$

and

$$ME_i = 1 - \frac{\sum_{j=1}^{n}\left(y_{ij} - y_{ij}^{*}\right)^2}{\sum_{j=1}^{n}\left(y_{ij} - \bar{y}_i\right)^2} \quad \text{(S30)}$$

in which i refers to data type (e.g., total body weight) and j to the individual measurements of the respective data type, y_{ij}; y_{ij}^{*} and $\bar{y}$ are values predicted by the (deterministic) model and mean of a data type, respectively. Overall goodness-of-fit measures were calculated by dividing the sum of corresponding goodness-of-fit measures for each data type by the number of data types.

SUPPLEMENTAL FIGURES

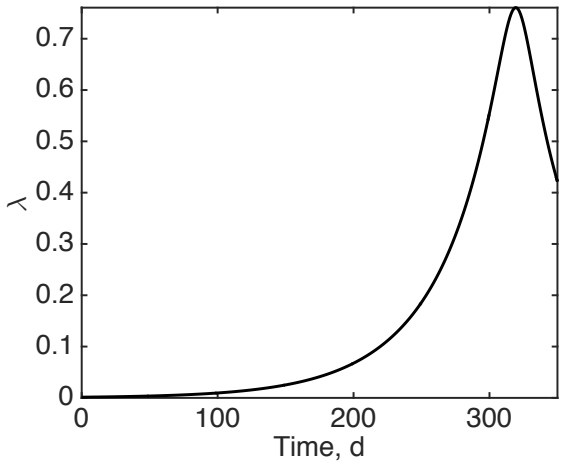

Figure S1. Time course of the fraction of somatic reserves allocated to reproduction in female rainbow trout in dDEB parameterized with the main data set. The mean fraction is 0.17.

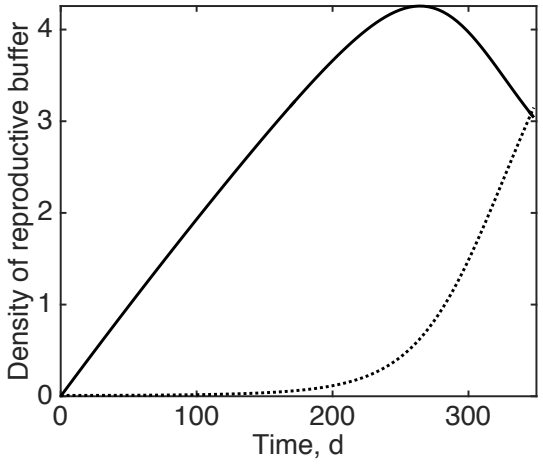

Figure S2. Density of reproductive reserves (solid curve) and actual reproductive matter (dotted curve) in female rainbow trout according to stdDEB+ parameterized with the main data set. At the time of spawning, only about 50% of the reproductive buffer, which is comprised of reproductive reserves and actual reproductive matter, is released in the form of eggs.

REFERENCES

Sale, P.J.M. (1975) Productivity of Vegetable Crops in a Region of High Solar Input. IV. Field Chamber Measurements on French Beans (Phaseolus vulgaris L.) And Cabbages (Brassica oleracea L.). *Australian Journal of Plant Physiology,* **2,** 461-470.